

## A TWO-SCALE CONSTITUTIVE PARAMETERS IDENTIFICATION PROCEDURE FOR ELASTO-PLASTIC FRACTURE

VALERIO CAROLLO, CLAUDIA BORRI AND MARCO PAGGI

IMT Institute for Advanced Studies Lucca, Research Unit MUSAM – Multi-scale Analysis of  
Materials, Piazza San Francesco 19, 55100 Lucca, Italy

e-mail: valerio.carollo@imtlucca.it, claudia.borri@imtlucca.it, marco.paggi@imtlucca.it

**Key words:** Computational Plasticity, Computational Fracture Mechanics, Elasto-plastic fracture.

**Abstract.** Constitutive parameters identification for elasto-plastic fracture is a complex problem due to the interplay between two forms of material nonlinearity, viz. plasticity and cohesive fracture. In the present study we examine this problem in relation to Copper specimens covered by Silver used in photovoltaic modules as electrical conductors. Uniaxial tensile tests on un-notched and notched specimens are performed with a tensile stage inside a scanning electron microscope, monitoring crack growth for each imposed far-field displacement. Parameters identification is then performed by considering an elasto-plastic constitutive relation with isotropic hardening for the continuum and a polynomial cohesive zone model (CZM) with two free parameters. For a better numerical-experimental fitting, a four-parameter CZM should be used to independently control the CZM stiffness and the fracture energy. To do so effectively, a constrained optimization procedure with a two-scale objective function is outlined.

### 1 INTRODUCTION

The identification of the constitutive parameters of the bulk and of the cohesive traction-separation law for cracks is a key issue for the reliability of numerical simulations of elasto-plastic fracture. Attempts to identify the cohesive zone model (CZM) parameters have been made in [1] by considering genetic algorithms and minimizing an objective function involving the global macroscopic response. As an alternative route, a method based on the J-integral has been proposed in [2] to identify the shape of the CZM by monitoring crack propagation in single-edge notched specimens tested inside a scanning electron microscope (SEM) chamber. The aim of the present study is to provide a novel identification procedure for the elasto-plastic constitutive parameters of the continuum and the shape of the CZM traction-separation relation via a two-scale approach.

The representative problem for elasto-plastic fracture addressed in the present study regards the mechanical behaviour of Silver-coated Copper conductors, also called busbars, used in the photovoltaic (PV) technology to electrically connect the solar cells inside the PV module. Typically, PV modules are made of polycrystalline or monocrystalline Silicon embedded in a polymer and covered by a glass layer. The surface of solar cells is covered by

fingers and busbars which respectively collect electrons and carry them through the neighbour cells connected them in series (see Fig. 1a). A detail of the gap between solar cells is shown in Fig. 1b.

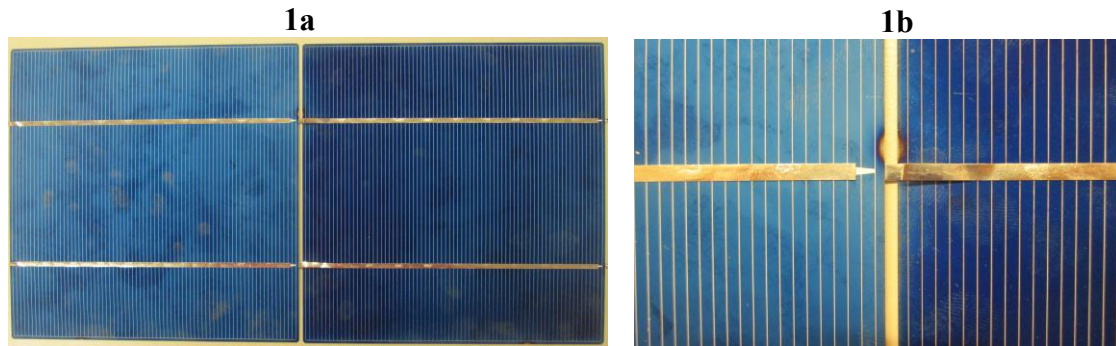


**Figure 1:** a) two adjacent cells connected by three busbars; b) detail of the gap between solar cells.

From the mechanical point of view, many factors can reduce the electric efficiency of solar cells. Recent research [3-5] shows that cracks can develop during transportation or installation of PV modules, not only during production. The crack pattern in the case of bending is also influenced by the load direction with respect to the busbars orientation [3]. The gap between connected cells is also a critical issue. The evolution of the relative displacement (gap) between two neighbour cells considering the mechanical properties of the thermo-viscoelastic envelop was investigated in [6]. Experimental data in Fig. 2 show that the gap width is strongly dependent on temperature and its variation can be as large as 60  $\mu\text{m}$  in the temperature range between  $-40\text{ }^{\circ}\text{C}$  and  $+85\text{ }^{\circ}\text{C}$ . Considering that the initial gap width is around 2 mm, the induced strain can lead to premature failure of the busbars, especially in the case of cycling thermal loads.

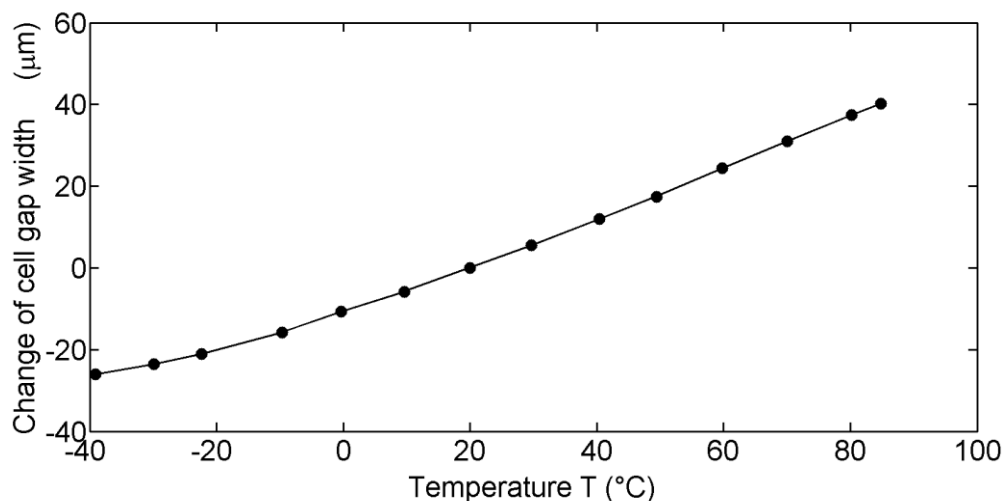


**Figure 2:** variation of the gap width between two adjacent solar cells vs. temperature.

In order to characterize elasto-plastic fracture in this mechanical system, a novel testing procedure is proposed in Section 2, and a general computational framework is presented in Section 3. The main problem of model parameters identification to quantitatively match the experimental results is finally addressed in Section 4.

## 2 EXPERIMENTAL TESTS

Experiments are conducted using a Deben Gatan MTEST5000S tensile stage (Fig. 3a) equipped with a 5 kN loading cell available in the MUSAM-Lab of the IMT Institute for Advanced Studied Lucca. The tensile stage is placed inside a scanning electron microscope (SEM) Zeiss EVO MA15, capable of working with variable pressure to avoid metallization or graphitization of the samples surface. This experimental setup allows performing monotonic and cyclic tensile tests and record images of the surface during the test at different magnifications, observing the evolution of crack propagation at the microscale. The tests have been performed by applying an axial displacement with constant velocity of 0.033 mm/min, see Fig. 4.

The busbars used for the experiments has a free span between clamps of 17 mm, a width of 2.6 mm and a thickness of 0.2 mm, see Fig. 3b. The busbar is a bi-material strip composed of an inner part of Copper, coated by a thin layer of Silver to reduce the electric resistance at the interface with the solar cell. In Fig. 3b it is possible to see this composition by etching the Silver coating in some areas.



**Figure 3:** a) tensile stage b) a busbar partially etched to show its bi-material composition.

Two type of experiments are performed. The first one is a tensile test on the un-notched busbar. The specimen is covered by Teflon at the clamps to avoid localized fracture there. A monotonically increasing axial displacement  $\Delta$  is applied (Fig. 4a). The main goal of this preliminary test is to analyze the elasto-plastic response of the material and identify the elastic parameters of the bi-material system, yield stress and its hardening coefficient during elasto-plastic deformation. As show in Fig. 5, results exhibit a clear elasto-plastic behavior with an approximately constant slope in both the elastic and the plastic regimes.

In the second type of experiments, the same test is conducted by using specimens with different notch lengths (Fig. 4b and 4c). The aim is to acquire data to be used for the

identification of the CZM parameters. Results show that the crack propagates only after achieving a considerable plastic deformation of the notch (Fig. 6). The corresponding force-displacement curve (Fig. 5) shows the appearance of a softening branch due to crack propagation. The longer the initial notch, the more premature is the specimen's failure.

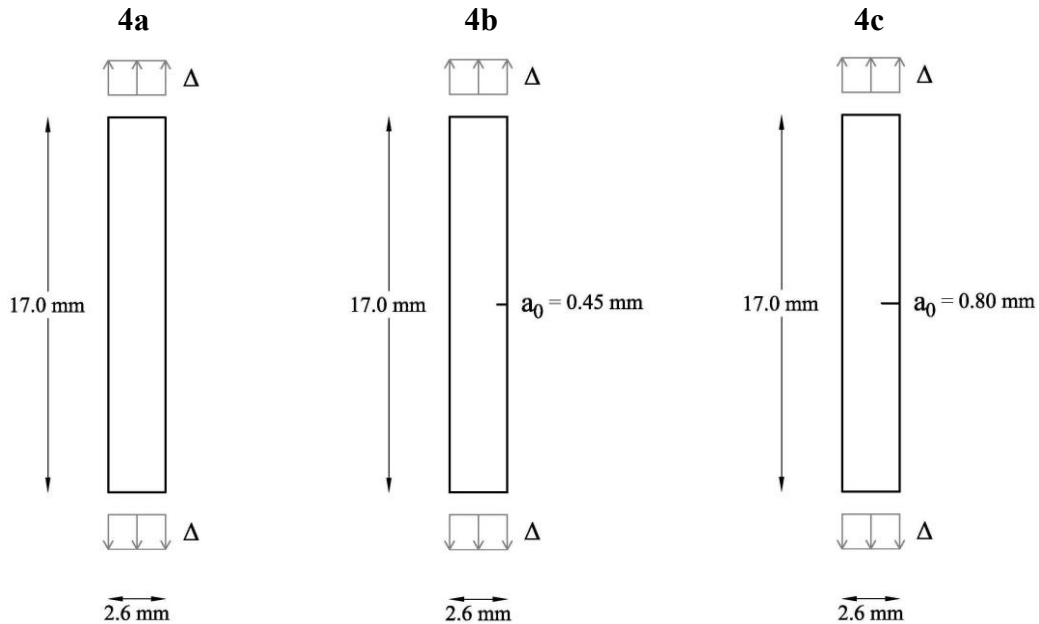


**Figure 4:** specimen geometry and loading condition.

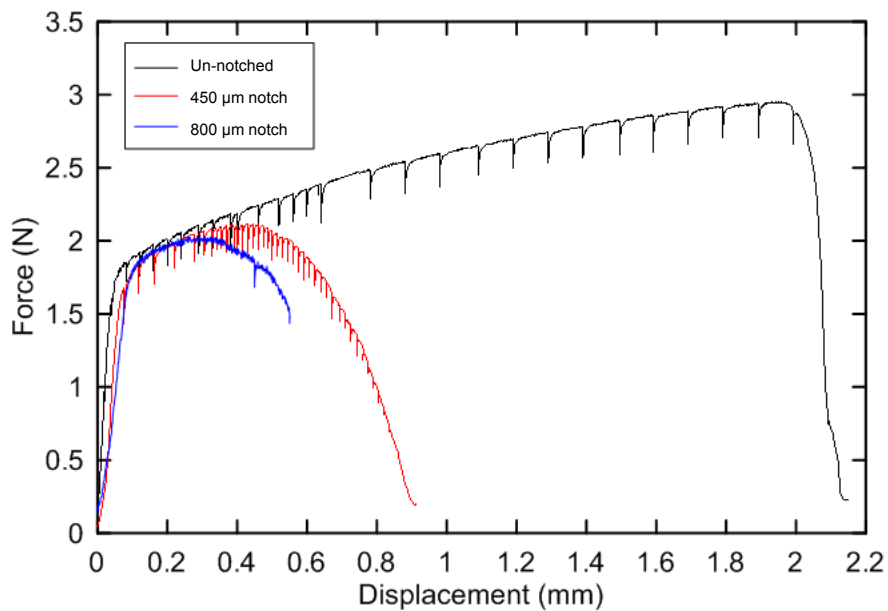


**Figure 5:** force-displacement curves of the tensile tests with a plain un-notched specimen or with an edge notch.

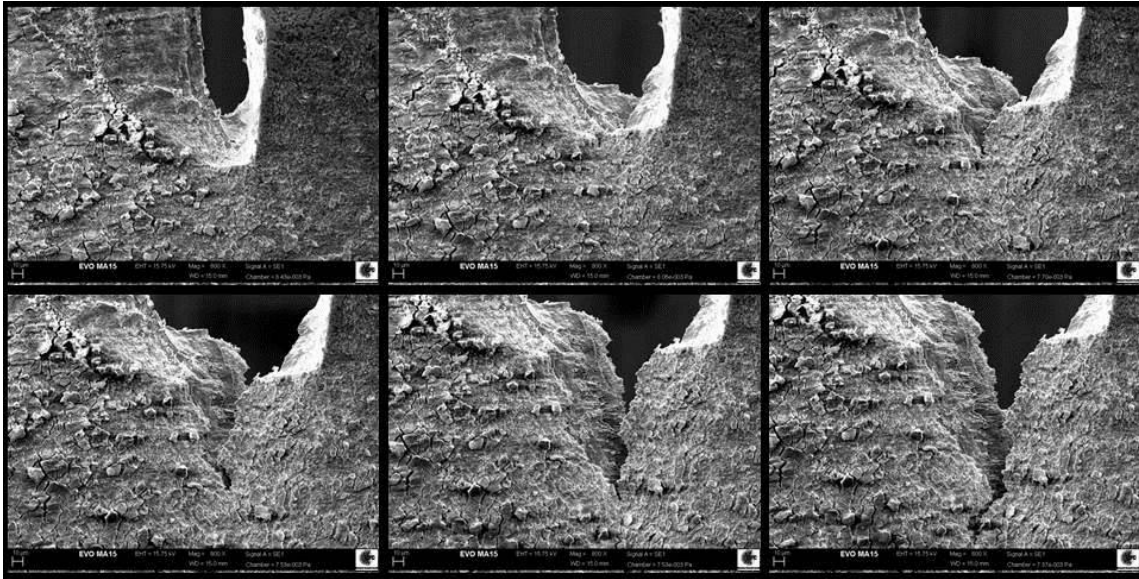


**Figure 6:** evolution of the crack opening near the notch for an increasing imposed axial displacement  $\Delta$ . From top left to right:  $\Delta = 0.163, 0.340, 0.415$  mm; from bottom left to right:  $\Delta = 0.445, 0.490, 500$  mm.

### 3 COMPUTATIONAL MODELLING AND PARAMETERS IDENTIFICATION

#### 3.1 Computational strategy and constitutive models

In order to simulate the phenomenon of elasto-plastic crack growth, we choose an elasto-plastic constitutive relation with isotropic hardening for the continuum:

$$\sigma = \begin{cases} E\varepsilon & \text{for } \sigma \leq \sigma_y \\ \sigma_y + H\varepsilon & \text{for } \sigma > \sigma_y \end{cases} \quad (1)$$

where  $\varepsilon$  is the total strain,  $\sigma$  is the axial stress,  $\sigma_y$  is the yield stress,  $E$  is the Young's modulus, and  $H$  is the isotropic hardening parameter. This constitutive model is already implemented in the finite element analysis program FEAP [7] which is used for the simulations performed according to an implicit (full Newton-Raphson) solution scheme. Regarding the FE discretization, we consider linear quadrilateral elements.

As far as crack propagation is concerned, the present problem is characterized by an *a priori* known crack path due to symmetry conditions. Therefore, 4-nodes interface elements implemented in the FE software FEAP [8] are inserted along the symmetry line in correspondence of the initial notch. Regarding the CZM constitutive relation, we preliminary consider the polynomial CZM in [9] where the Mode I cohesive traction  $\sigma$  is a function of the crack opening  $g_n$  as follows:

$$\sigma = \begin{cases} \sigma_{\max} \frac{g_n}{g_c} \frac{27}{4} \left[ 1 - 2 \left( \frac{g_n}{g_c} \right) + \left( \frac{g_n}{g_c} \right)^2 \right] & \text{for } 0 \leq \frac{g_n}{g_c} < 1 \\ 0 & \text{for } \frac{g_n}{g_c} \geq 1 \end{cases} \quad (2)$$

Hence, the application of the present constitutive equations requires the identification of five parameters, namely the Young's modulus  $E$ , the yield stress  $\sigma_y$ , the hardening parameter  $H$ , the maximum cohesive traction  $\sigma_{\max}$ , and the critical opening displacement  $g_c$ .

### 3.2 Elasto-plastic parameters identification

As mentioned in the previous section, the parameters describing the material properties of the bulk are the Young's modulus  $E$ , the yield stress  $\sigma_y$ , and the hardening coefficient  $H$ , while we set equal to zero the Poisson's ratio for the sake of simplicity, since its value is slightly affecting the mechanical response. The experimental data of the tensile test on the unnotched specimen are well represented by a bilinear stress-strain curve, see Fig. 7. The Young's modulus can be estimated by a linear best-fitting of the stress-strain curve in the strain range from zero up to 0.2%, leading to  $E=1314$  MPa. On the other hand, a linear best-fitting on the plastic part of the diagram approximately from 0.4% up to 1.1% leads to the yield stress  $\sigma_y=3.55$  MPa and the hardening coefficient  $H=18.06$  MPa. A comparison between the experimental stress-strain curve (in black) and the identified bi-linear one (in red) is shown in Fig.7.

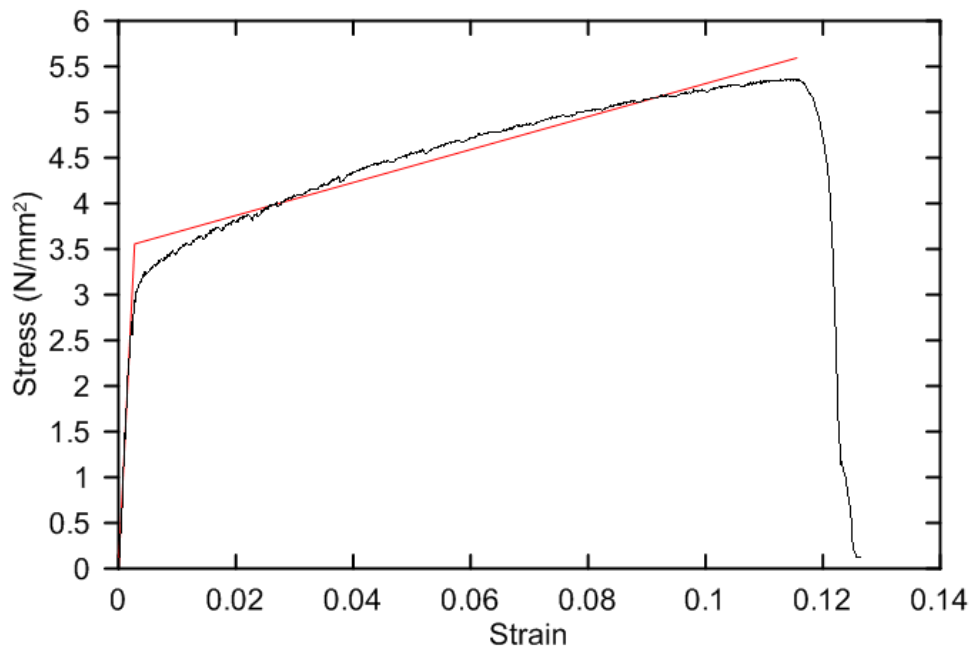


**Figure 7:** experimental stress-strain curve and its bilinear approximation.

### 3.3 CZM parameters identification

Considering a notched specimen subject to uniaxial tension with an initial notch size  $a_0=450 \mu\text{m}$ , the maximum cohesive traction and the critical opening displacement can be identified from a series of parametric simulations by varying the free parameters entering the CZM and keeping constant the elasto-plastic material parameters previously identified. The FE mesh, consisting in linear quadrilateral elements and 4-nodes interface elements, is shown in Fig. 8a, while the deformed mesh with the superimposed contour plot of the axial displacement field component in correspondence of  $\Delta=1 \text{ mm}$  is shown in Fig. 8b. The axial stress field is shown in the contour plot in Fig. 8c.

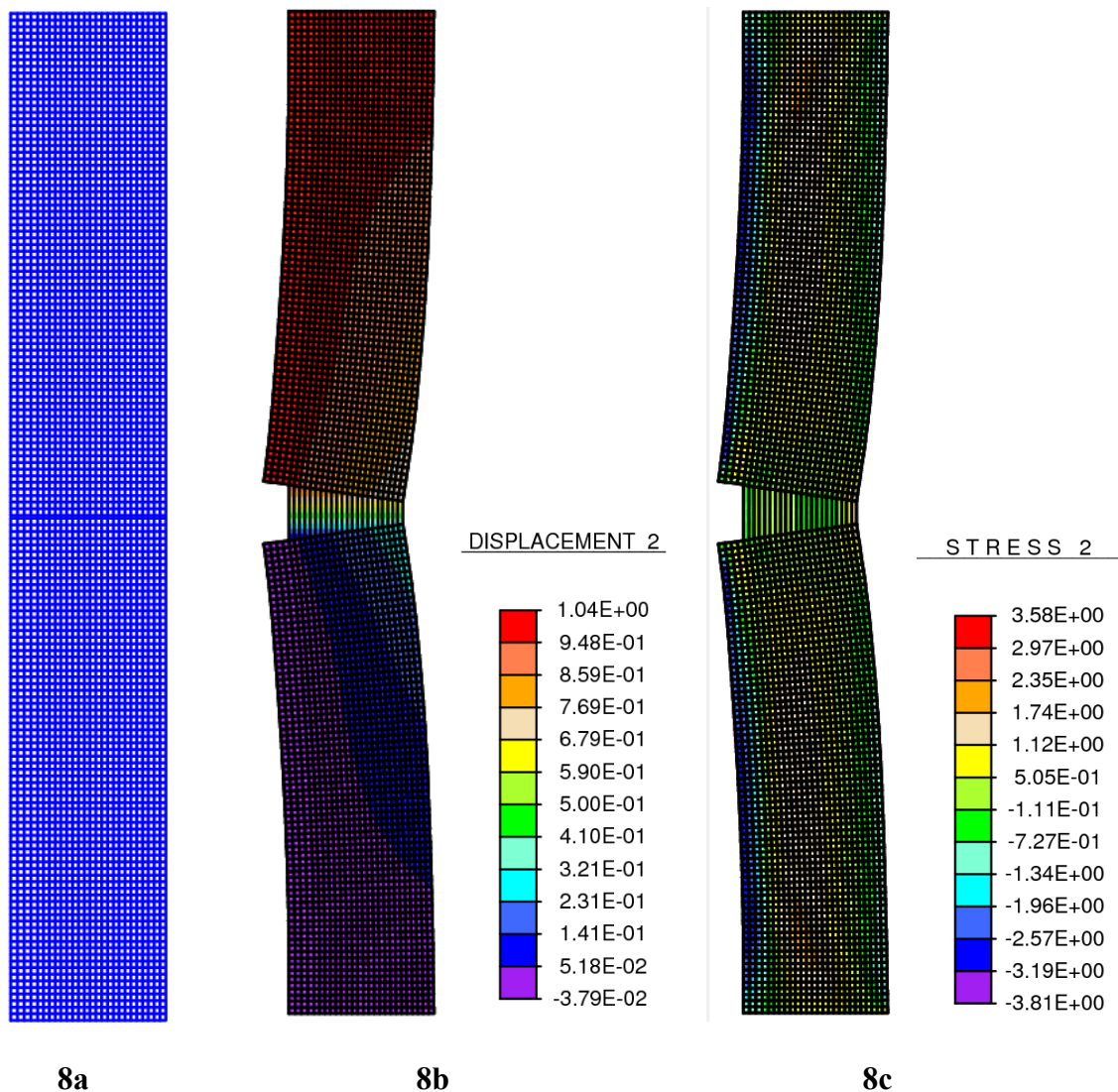
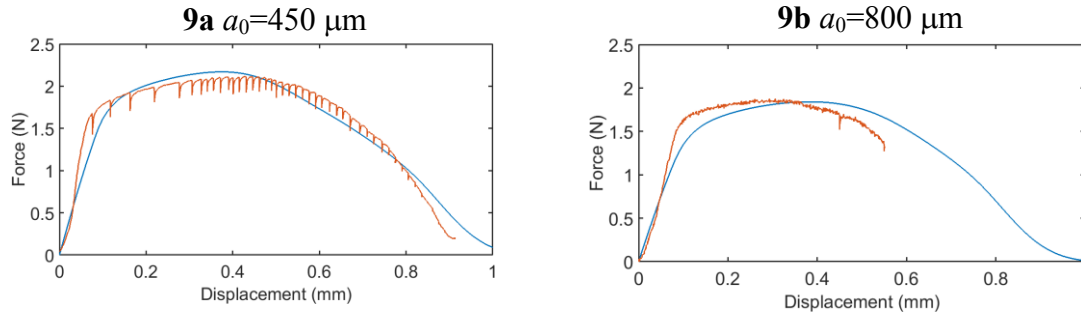


Figure 8: FE model of the notched busbar tested in uniaxial tension.



After extensive testing, the best agreement between the numerical predictions and the experimental results in terms of axial force vs. axial displacement is obtained for  $\sigma_{\max} = 6.5$  MPa and  $g_c = 0.5$  mm, see Fig. 9a.

However, the use of the same CZM parameters to simulate the sample with  $a_0=800$   $\mu\text{m}$  does not provide a good matching with experiments (Fig. 9b). The reason for that could be related to the fact that the slope of the CZM for low  $g_n$  has a role and it cannot be varied independently from the fracture energy in the Tvergaard CZM.



**Figure 9:** experimental force-displacement curve in red and the numerical simulation in blue.

#### 4 A TWO-SCALE IDENTIFICATION PROCEDURE

A better procedure for the identification of the CZM parameters can be carried out by considering a more general Mode I  $\sigma$  vs.  $g_n$  traction-separation relation with four free parameters, namely the initial slope,  $k$ ; the maximum traction,  $\sigma_{\max}$ ; the separation corresponding to the maximum traction,  $g_m$ ; and the critical separation,  $g_c$ . the imposition of these conditions on a polynomial form leads to a fifth order polynomial equation with four free parameters:

$$\sigma = \begin{cases} \frac{g_n}{g_m^2} (g_n - g_c)^2 \left[ \left( \frac{k}{g_c^2} + \frac{2\sigma_{\max}(g_c - 2g_m)}{g_m(g_m - g_c)^3} \right) g_n^2 + \left( \frac{5\sigma_{\max}g_m - 3\sigma_{\max}g_c}{(g_m - g_c)^3} - \frac{2kg_m}{g_c^2} \right) g_n + \frac{kg_m^2}{g_c^2} \right] & \text{for } 0 \leq g_n \leq g_c \\ 0 & \text{for } g_n \geq g_c \end{cases} \quad (3)$$

Eq. (3) allows a tuning of the initial slope of the traction-separation relation for a vanishing cohesive traction and of the fracture energy independently from each other, which is not possible with the Tvergaard CZM [9] used in section 3. Moreover, the Tvergaard CZM is a special case of Eq. (3) when the term in square brackets is a constant suitably chosen to obtain the expression in Eq. (2).

Based on this formulation, a parameter identification with four free parameters is hard to be carried out manually. Therefore, an optimization procedure is suggested by considering an objective function  $\Phi$  to be minimized, defined as the sum of two norms that measure the distance between the numerical predictions and the experimental results. The former involves the parameters related to the microscopic response such as the crack opening and the real crack length that can be measured from SEM images, whereas the latter regards macroscopic data such as the force-displacement response. Hence, under these assumptions the



unconstrained convex objective function reads:

$$\Phi = \alpha \left\| P_{\text{micro}}^{(\text{num})} - P_{\text{micro}}^{(\text{exp})} \right\| + \beta \left\| P_{\text{macro}}^{(\text{num})} - P_{\text{macro}}^{(\text{exp})} \right\| \quad (4)$$

where  $0 \leq \alpha \leq 1$  and  $0 \leq \beta \leq 1$  ( $\alpha + \beta = 1$ ) are two weights used to give different priority to the micro or to the macro-scale responses  $P_{\text{micro}}$  or  $P_{\text{macro}}$  during the identification procedure. A further complexity arises by the fact that the free parameters have to satisfy a set of inequalities in order to provide a CZM relation physically admissible, i.e.:

$$\begin{aligned} 0 < g_m < g_c \\ \sigma_{\text{max}} > \sigma_y \\ k > \sigma_{\text{max}}/g_m \end{aligned} \quad (5)$$

Hence, a constrained optimization has to be carried out by including the constraints and the unconstrained objective function in a suitable Lagrangian formulation [10]. Since the Lagrangian is computed numerically, the derivatives of the Lagrangian with respect to the free parameters to be identified and with respect to the Lagrange multipliers have also to be determined numerically.

## 5 CONCLUSIONS

In the present study, the constitutive parameters for elasto-plastic fracture of Silver coated Copper electric conductors used in photovoltaic modules have been identified based on experimental tests carried out inside a scanning electron microscope. A standard identification procedure provides a fair good agreement between numerical predictions and experimental results. Further improvement is indeed possible and it requires more than two free parameters to define the cohesive traction-separation relation. In this case, parameters identification cannot be carried out manually and an optimization procedure is required. To avoid unphysical solutions, a two-scale constrained optimization procedure is outlined. Further work will regard the implementation of the optimization procedure and its application to specimens tested in tension with different notch depths in order to determine notch size-independent CZM parameters.

## ACKNOWLEDGEMENTS

The research leading to these results has received funding from the European Research Council under the European Union's Seventh Framework Programme (FP/2007–2013)/ERC Grant Agreement No. 306622 (ERC Starting Grant “Multi-field and Multi-scale Computational Approach to Design and Durability of PhotoVoltaic Modules” – CA2PVM).

## REFERENCES

- [1] Valoroso, N. and Fedele, R. *Characterization of a cohesive-zone model describing damage and de-cohesion at bonded interfaces. Sensitivity analysis and mode-I parameter identification*. International Journal of Solids and Structures, 47, (2010) 1666-1677.
- [2] Desay, C.K., Kumar, A.S., Basu, S. and Parameswaran, V. *Measurement of cohesive parameters of crazes in polystyrene films*. Experimental and Applied Mechanics, 6, (2011).
- [3] Sander, M., Dietrich, S., Pander, M., Ebert, M. and Bagdahn, J. *Systematic investigation of cracks in encapsulated solar cells after mechanical loading*. Solar Energy Materials & Solar Cells 111 (2013) 82–89.
- [4] Infuso, A., Corrado, M. and Paggi, M. *Image analysis of polycrystalline solar cells and modeling of intergranular and transgranular cracking*. Journal of the European Ceramic Society 34 (2014) 2713–2722.
- [5] Paggi, M., Berardone, I., Infuso, A. and Corrado, M. *Fatigue degradation and electric recovery in Silicon solar cells embedded in photovoltaic modules*. Scientific Report 4 (2014) 4506.
- [6] Paggi, M., Kajari-Schoeder, S. and Eitner, U. *Thermomechanical deformations in photovoltaic laminates*. The Journal of Strain Analysis for Engineering Design 46 (2011) 772.
- [7] Zienkiewicz, O.C. and Taylor, R.L. *The finite element method*. McGraw Hill, Vol. I., (1989), Vol. II, (1991).
- [8] Paggi, M. and Wriggers, P. *A nonlocal cohesive zone model for finite thickness interfaces – Part II: FE implementation and application to polycrystalline materials*. Computational Materials Science 50 (2011) 1634–1643
- [9] Tvergaard, V. *Effect of fiber debonding in a whisker-reinforced metal*. Materials Science and Engineering A 107 (1990) 23-40.
- [10] Boyd, S. and Vandenberghe, L. *Convex optimization*. Cambridge University Press 2004.